Conference Proceedings of the Society for Experimental Mechanics Series

Gary L. Cloud · Eann Patterson · David Backman *Editors*

Joining Technologies for Composites and Dissimilar Materials, Volume 10

Proceedings of the 2016 Annual Conference on Experimental and Applied Mechanics

SEM

Springer

Conference Proceedings of the Society for Experimental Mechanics Series

Series Editor

Kristin B. Zimmerman, Ph.D.
Society for Experimental Mechanics, Inc
Bethel, CT, USA

More information about this series at http://www.springer.com/series/8922

Gary L. Cloud • Eann Patterson • David Backman
Editors

Joining Technologies for Composites and Dissimilar Materials, Volume 10

Proceedings of the 2016 Annual Conference on Experimental and Applied Mechanics

Springer

Editors
Gary L. Cloud
Composite Vehicle Research Center
Michigan State University
Lansing, MI, USA

David Backman
National Research Council Canada
Ottawa, ON, Canada

Eann Patterson
University of Liverpool
Liverpool, UK

ISSN 2191-5644 ISSN 2191-5652 (electronic)
Conference Proceedings of the Society for Experimental Mechanics Series
ISBN 978-3-319-42425-5 ISBN 978-3-319-42426-2 (eBook)
DOI 10.1007/978-3-319-42426-2

Library of Congress Control Number: 2012943040

Printed on acid-free paper

This Springer imprint is published by Springer Nature
The registered company is Springer International Publishing AG Switzerland

Preface

Joining Technologies for Composites and Dissimilar Materials represents one of ten volumes of technical papers presented at the 2016 SEM Annual Conference & Exposition on Experimental and Applied Mechanics organized by the Society for Experimental Mechanics and held in Orlando, FL, on June 6–9, 2016. The complete Proceedings also includes volumes on *Dynamic Behavior of Materials; Challenges in Mechanics of Time-Dependent Materials; Advancement of Optical Methods in Experimental Mechanics; Experimental and Applied Mechanics; Micro and Nanomechanics; Mechanics of Biological Systems and Materials; Fracture, Fatigue, Failure and Damage Evolution; and Residual Stress, Thermomechanics & Infrared Imaging, Hybrid Techniques and Inverse Problems.*

Composite materials are being increasingly utilized at multiple levels in application areas including automotive, aerospace, marine, biomechanical, and civil infrastructure, so the need for improved joining of these materials has become critical. While the design of the composite laminate is important, it is the ability to join sections of composite to one another or to components made of dissimilar materials that is the enabling technology for creating structures that approach optimum in function, weight, durability, and cost.

Composite joining technologies have been routinely classified in the past as either mechanical or adhesive. Increasingly, joint optimization requires combinations of the two types as well as the introduction of innovative new methods, such as composite welding, that provide high strength and light weight. Hybrid composite joints that allow the joining of composites to monolithic or other classes of material comprise another important technology that will facilitate the use of composites in many new application areas. Today, developments in composite joining technologies are progressing at a rapid rate, driven by both technology and user requirements.

This symposium addresses pertinent issues relating to design, analysis, fabrication, testing, optimization, reliability, and applications of composite joints, especially as these issues relate to experimental mechanics of macroscale and microscale structures.

East Lansing, MI, USA — Gary L. Cloud
Liverpool, UK — Eann A. Patterson
Ottawa, ON, Canada — David Backman

Contents

Chapter 1
How to Join Fiber-Reinforced Composite Parts: An Experimental Investigation

Yaomin Dong, Arnaldo Mazzei, Javad Baqersad, and Azadeh Sheidaei

Abstract A coupler has been developed to prevent windshield wiper systems from being damaged by excessive loads that can occur when the normal wiping pattern is restricted. Unlike the traditional steel coupler used in wiper systems, the composite coupler will buckle at a prescribed compressive load threshold and become extremely compliant. As a result, the peak loading of the coupler and the entire wiper system can be greatly reduced. The coupler is composed of a pultruded composite rod with injection-molded plastic spherical sockets attached at either end. The sockets are used to attach the coupler to the crank and rocker of the windshield wiper linkage. Because the loads exerted on a coupler vary in magnitude and direction during a wiping cycle, the joint between the sockets and the pultruded composite rod must be robust. The paradigm for attaching sockets to steel couplers (i.e. over-molding the sockets around holes stamped into the ends of traditional steel couplers) was tested and found to produce inadequate joint strength. This paper details the methodology that was employed to produce and optimize an acceptable means to join the injection-molded sockets to the fiber glass pultruded rods. Specifically, a designed experiment based on the Robust Design Strategy of Taguchi was used to identify the process, processing parameters, and materials that yield a sufficiently strong joint at a reasonable manufacturing cost without damaging the integrity of the underlying composite structure.

Keywords Composite materials • Buckling • Wiper systems • Durability • Joint strength

1.1 Introduction

Automotive windshield wiper systems, in conjunction with washer systems, are used in vehicles to remove contaminants such as rain, sleet, snow, and dirt from the windshield. As shown in Fig. 1.1, a typical wiper system consists of an electric motor, a linkage to transform the rotational motion from the motor to oscillatory motion, and a pair of wiper arms and blades. The areas of the windshield that must be wiped by the wiper system are mandated by the federal motor vehicle safety standards FMVSS 104 [1].

Figure 1.2 shows that snow has accumulated above the cowl screen and caused the normal wiping pattern of the system to be restricted. Under such conditions, the loads in the wiper system have been observed to be approximately four times greater than those encountered under normal wiping conditions for a particular application. The elevated loads are due to two factors: (1) As the arm(s) and/or blade(s) come into contact with the restriction, the speed of the wiper system decreases and the output torque of the motor increases. (2) This factor is aggravated by the very large mechanical advantage of the wiper linkage near the reversal positions.

In extreme cases, the loads that result from restricting the wipe pattern can cause failures. For example, Fig. 1.3 depicts a 5-mm thick hardened steel rocker arm that has fractured as a result of such a loading. Clearly, such a damage is unacceptable from both safety and warranty standpoints.

Penrod and Dong [2] reviewed various methods that have been developed to solve this problem. One such solution is to use a coupler fabricated from a thermoset polyester/glass fiber pultruded composite material [3–6]. This coupler—referred to as the composite link—has the advantage of being sufficiently stiff during normal operation providing very good pattern control. However, in the event that elevated loads occur, the coupler is designed to buckle at a prescribed load level (i.e. the critical load). Once buckled, the coupler becomes extremely compliant. As a result, the peak loading of the coupler and, moreover, the entire system, can be limited and greatly reduced when compared to the same system without the composite link.

Y. Dong, Ph.D. (✉) • A. Mazzei, Ph.D. • J. Baqersad, Ph.D., P.E. • A. Sheidaei, Ph.D.
Department of Mechanical Engineering, Kettering University, 1700 University Avenue, Flint, MI 48504-4898, USA
e-mail: ydong@kettering.edu

G.L. Cloud et al. (eds.), *Joining Technologies for Composites and Dissimilar Materials, Volume 10*
Conference Proceedings of the Society for Experimental Mechanics Series, DOI 10.1007/978-3-319-42426-2_1

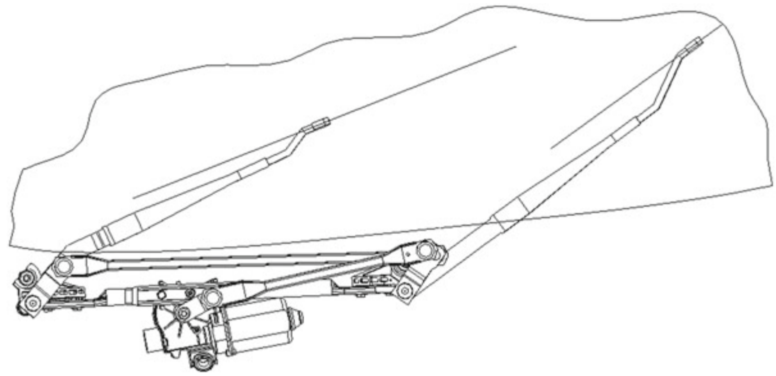

Fig. 1.1 A typical wiper system consists of wipers, motor, and a linkage, and wiper arms

Fig. 1.2 Restricted wiping pattern due to snow accumulation

Fig. 1.3 Fractured rocker arm resulting from snow accumulation

Figure 1.4 shows the operating principle of the composite link. In the illustration the wiper arms have encountered snow/ice accumulation (depicted by the hatched pattern) above the cowl screen that blocks the normal wiping pattern of the system. As a result, the wiper system loads have increased sufficiently to buckle the composite link (depicted by the arcuate member

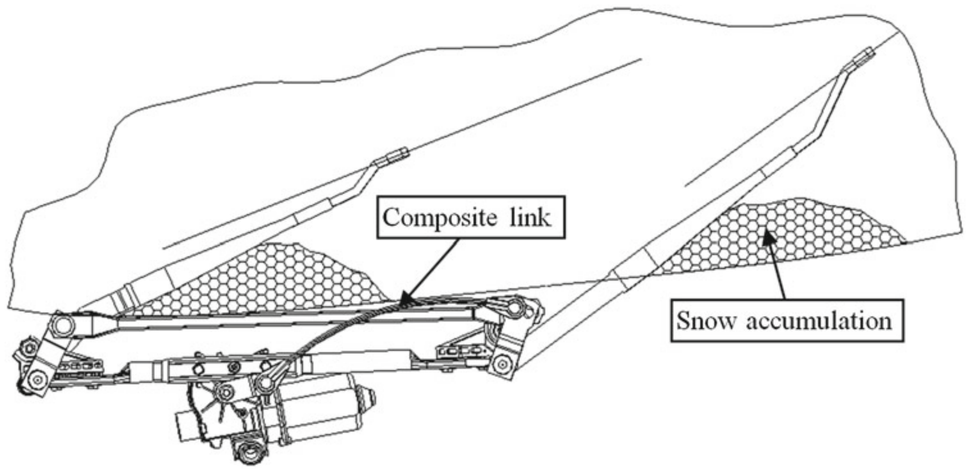

Fig. 1.4 Operating principle of the composite link

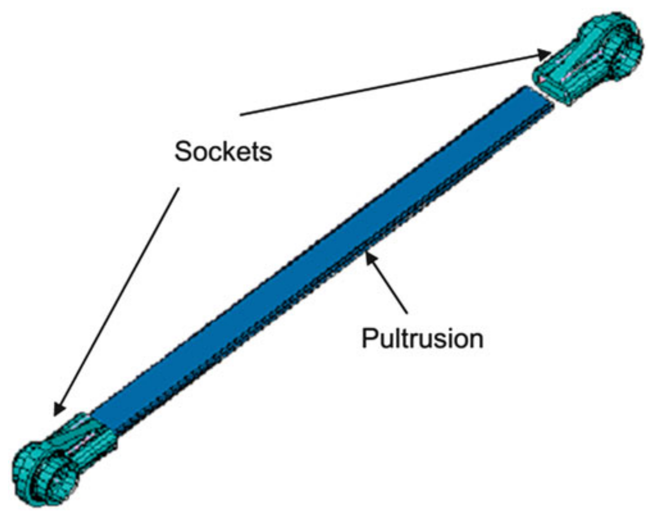

Fig. 1.5 Composite link assembly

of the wiper linkage). Once buckled, the composite link behaves nearly perfectly-plastic. As a result, the chord length of the composite link decreases significantly without a corresponding appreciable increase in axial load. Thus the crank is able to continue rotating and the wiper system is enabled to wiper at a reduced area above the restriction.

The composite link is an assembly of a 16.7 mm × 5.2 mm rectangular cross-section pultrusion and glass-filled plastic sockets attached at either end, as shown in Fig. 1.5. The design methodology, material selection, validation testing, and application guidelines for the composite link are discussed in detail by Penrod, Dong, and Buchanan [3]. Because the loads exerted on the coupler vary in magnitude and direction during each wiping cycle, the joint between the sockets and the pultrusion is critical and must be robust.

Initially, it was planned to attach the sockets to the pultrusion rod using the same approach that sockets have been traditionally joined to steel couplers (i.e. over-molding the sockets around holes stamped into the ends of the traditional steel coupler). In the case of the composite link, holes were drilled into the ends of the pultrusion and the sockets were over-molded onto the pultrusions. Unfortunately, this joining method performed dismally as it was characterized by bearing stress failures of the pultrusion at relatively low tensile loads. In retrospect, this failure mode was no surprise. The pultrusions consist of longitudinally oriented continuous glass fibers bound together by a thermosetting polyester matrix. Drilling holes on the pultruded rod cuts the continuous fibers and weakens the composite structure. As such, the material has little strength on short-transverse planes where the bearing failure was observed to occur.

Since the paradigm for attaching sockets to steel links did not work, a Greenfield approach to attaching sockets to the pultrusions was embarked upon. This paper details the approach that was employed to generate, evaluate, and optimize an acceptable means of attaching the injection-molded plastic sockets to the pultrusions.

1.2 Designed Experiment for Joining Socket to Pultrusion

How can the plastic sockets be attached to the pultruded composite rod? The traditional approach of over-molding the sockets to steel links proved inadequate as was discussed previously. In order to answer this question, a set of design specifications were generated to assess design concepts against. Qualitatively, the specifications of paramount importance were that the attachment method.

- Provide adequate joint strength in tension and compression when subjected to monotonic and cyclic loads.
- Avoid damaging the integrity of the glass fibers to the extent that the pultrusion would no longer be capable of providing a predictable critical load and adequate post-buckled axial compressive deflection.
- Be cost-effective.

Once the aforementioned specifications were established, three phases of the development were sequentially undertaken. Specifically,

- *System Design*: the first phase of the development where a variety of state-of-the-art candidate processes were generated using input from a cross-functional team of material, manufacturing, and product specialists. Once identified, the candidate processes were then narrowed to the most promising approaches via conceptual evaluation by the cross-functional team. Additionally, some ad hoc testing was completed in this phase of the development that suggested adding grooves to the ends of the pultrusion so that the over-molded socket could form a positive lock was the most viable approach.
- *Parameter Design*: the second phase of the development where a series of designed experiments were used to quantitatively ascertain the optimal combination of design and processing parameters.
- *Tolerance Design*: the third and final phase of the development where the allowable tolerance range on the critical dimensions and processing parameters were determined.

The focus of this paper is on the series of designed experiments that were used to identify the optimal combination of designs, materials, and processes during the parameter design phase of the development.

1.2.1 Parameter Selection Stage 1: Screening

The Robust Design Strategy of G. Taguchi [7] has gained broad acceptance in Japan, the United States, and elsewhere for use in product design and development. Taguchi's approach to parameter design provides a systematic and efficient method for determining near-optimum design parameters. The Taguchi method allows for the sensitivity of the design to a large number of parameters to be evaluated using a relatively small number of sample parts by utilizing orthogonal arrays from design of experiments theory. The conclusions drawn from such small scale experiments are valid over the entire experimental range spanned by the control factors and control factor levels.

As mentioned previously, adding grooves to the pultrusion ends so that the over-molded socket would be positively locked to the pultrusion was deemed the most viable approach. However, the influence of other factors on the joint strength was still unknown. Specifically, what is the influence of the surface finish of the pultrusion on joint strength? What role does the location of the grooves play? Does the socket material significantly impact the joint strength? What benefit might be derived from the use of adhesives? What is the influence of glass content in the pultrusion on joint strength? To answer these questions, an experiment was designed to screen these factors for relative importance and identify where the various factors might interact—both in a positive and negative sense.

Table 1.1 depicts the L18 Orthogonal Array that was used to screen the design candidates. Notice that the five aforementioned design parameters (A ~ F) are chosen as control factors, with each factor having three levels. Descriptions of the control levels indicated in the array are as follows.

- Surface Finish: Smooth denotes the surface finish of the pultrusion without any additional processing. Abrasive-fine, and abrasive-coarse denote that the ends of the pultrusion have been grit blast with a fine and coarse medium, respectively. Chemical etched refers to the resin-rich surface of the pultrusion ends being removed using an acidic solution. Laser etches #1 and #2 denote two power levels used to remove the resin-rich surface of the pultrusion via the use of a laser.
- Machined Grooves: Smooth denotes no grooves, top–bottom denotes grooves machined into the top and bottom surfaces of the pultrusions. Side-side denotes grooves machined into the edges of the pultrusions. Ultimately, axial grooves which

Table 1.1 L18 Orthogonal array for stage 1 (screening)

	1&2	3	4	5	6
	A	B	D	E	F
	Surface finish	Machined grooves	Socket material	Attachment/adhesives	Pultrusions
1	Smooth	Smooth	Nylon	Insert mold/hot curing	Low modulus
2	Smooth	Top-bottom	Acetal #1	Mech attach/chem. cure	Moderate modulus
3	Smooth	Side-side	Acetal #2	Insert mold/no adhesive	High modulus
4	Abrasive-fine	Smooth	Nylon	Mech attach/chem. cure	Moderate modulus
5	Abrasive-fine	Top-bottom	Acetal #1	Insert mold/no adhesive	High modulus
6	Abrasive-fine	Side-side	Acetal #2	Insert mold/hot curing	Low modulus
7	Abrasive-coarse	Smooth	Acetal #1	Insert mold/hot curing	High modulus
8	Abrasive-coarse	Top-bottom	Acetal #2	Mech attach/chem. cure	Low modulus
9	Abrasive-coarse	Side-side	Nylon	Insert mold/no adhesive	Moderate modulus
10	Chemical etch	Smooth	Acetal #2	Insert mold/no adhesive	Moderate modulus
11	Chemical etch	Top-bottom	Nylon	Insert mold/hot curing	High modulus
12	Chemical etch	Side-side	Acetal #1	Mech attach/chem. cure	Low modulus
13	Laser etch #1	Smooth	Acetal #1	Insert mold/no adhesive	Low modulus
14	Laser etch #1	Top-bottom	Acetal #2	Insert mold/hot curing	Moderate modulus
15	laser etch #1	Side-side	Nylon	Mech attach/chem. cure	High modulus
16	Laser etch #2	Smooth	Acetal #2	Mech attach/chem. cure	High modulus
17	Laser etch #2	Top-bottom	Nylon	Insert mold/no adhesive	Low modulus
18	Laser etch #2	Side-side	Acetal #1	Insert mold/hot curing	Moderate modulus

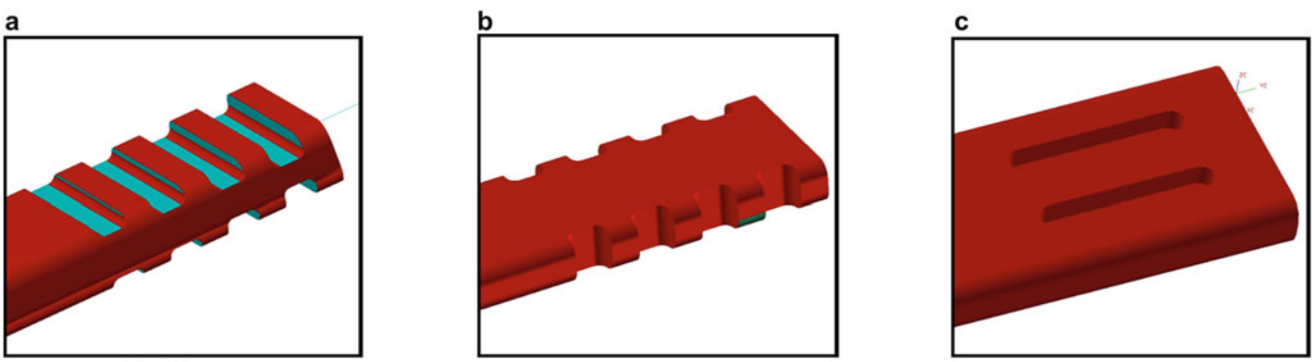

Top-Bottom Side-Side Axial

Fig. 1.6 Groove configurations

are oriented longitudinally were also considered. (Please see Sect. 2.3 for details.) All grooves were full-filleted as indicated in Fig. 1.6 and were machined by grinding.

- Socket Material: Nylon denotes a glass-filled nylon 6/6. Acetal #1 refers to 20 % glass-filled acetal, whereas acetal #2 refers to 30 % glass-filled acetal.
- Attachment/adhesives: Three possibilities were considered. Insert molding the sockets over the ends of the pultrusion was done both without adhesives (i.e. insert mold/no adhesive) and with adhesives (i.e. insert mold/hot curing). Hot curing refers to the heat available from the injection molded material promoting rapid curing of the adhesive.) Mechanical attachment of the socket to the pultrusion was also considered and used an adhesive to bond the sockets to the pultrusions. In this case an accelerant was used to promote curing of the adhesive. Thus, this approach is denoted by mech attach/chem cure in Table 1.1. In all cases, the adhesive used was a commercially available cyanoacrylate.
- Pultrusions: Low-, moderate-, and high-modulus refer to elastic modulus of the pultusions resulting from three different glass content levels being used. The higher the glass content, the higher the modulus.

It should be noted that a full-factorial experiment would require evaluating the performance of ($6 \times 3 \times 3 \times 3 \times 3 =$) 486 combinations of control factors and control levels. Using the Taguchi approach, only 18 combinations need to be considered with the 18 specific combinations of control factors and control levels dictated by the method.

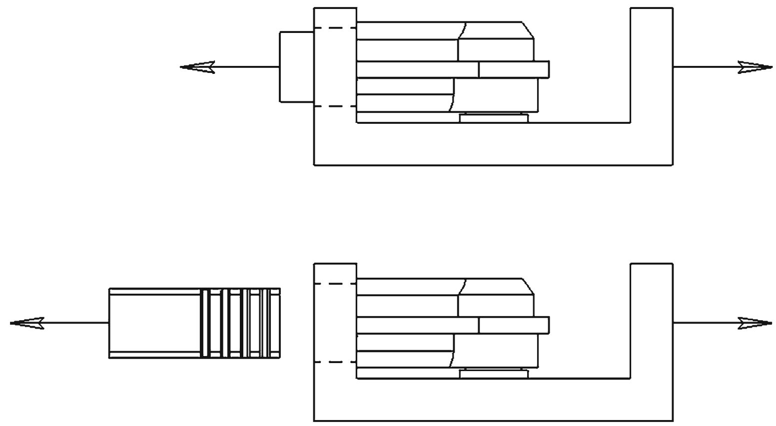

Fig. 1.7 Strip test used to determine the ultimate strength of the joint

Table 1.2 L9 Orthogonal array for stage 2 (groove design)

	1	2	3
	A	B	C
	Groove size	Groove spacing	Number of grooves
1	Small	#1	Few
2	Small	#2	Moderate
3	Small	#3	Many
4	Medium	#1	Moderate
5	Medium	#2	Many
6	Medium	#3	Few
7	Large	#1	Many
8	Large	#2	Few
9	Large	#3	Moderate

Once the 18 combinations were prototyped, a strip test was run on each configuration to determine the ultimate strength of each joint in tension. Figure 1.7 depicts the test. The assembled composite link was placed in a specially designed fixture that captured the socket only. The tensile load was increased until the assembly of the socket and pultrusion separated. Analyzing the data collected from the testing using the Taguchi approached allowed for the contribution to the joint strength of each control factor and control level, and interactions of the control factors and control levels to be quantified. From this analysis, it was found that grooves added to the top and bottom faces of the pultrusion were the single greatest contributor to joint strength. The use of adhesives to produce bonding between the socket and pultrusion was found to be the second largest contributor to strength, but was ruled out due to processing difficulties. Additionally, altering the surface finish of the pultrusion provided little benefit and was quite costly. As such, it was also disqualified from further consideration.

1.2.2 Parameter Selection Stage 2: Groove Design

Based on the results of the screening designed experiment, a second designed experiment was constructed to further optimize the groove design. Table 1.2 depicts the L9 Orthogonal Array that was constructed for this purpose. In this experiment three control factors (i.e. groove size, groove spacing, and number of grooves) were considered at three different control levels. Once again it is noteworthy that the number of configurations to be tested is only nine and that a full factorial experiment would require 27 (i.e. $3 \times 3 \times 3$) configurations.

The control levels indicated in Table 1.2 are described as follows.

- Groove Size: Small denotes 0.5 mm depth, while medium corresponds to 1.0 mm depth, and large denotes a 1.5 mm depth.
- Groove Spacing: The spacing between adjacent grooves with level #1 corresponding to 2 mm spacing, level #2 corresponding to 3 mm spacing, and level #3 corresponding to 4 mm spacing.
- Number of Grooves: Few denotes two grooves per face, moderate denotes four grooves per face; and many corresponding to six grooves per face.

Prototype parts of each configuration were fabricated and evaluated against two criteria. The first criterion was simply evaluating the tensile strength of the joint as was performed in the screening experiment. The second criterion involved examining the performance of the composite links in compression after being buckled and axially compressed to a preset deflection. Doing so revealed that under certain circumstances, the pultruded material tends to delaminate on long-transverse planes with the delamination initiating at the root of the groove.

Analyzing the data using the Taguchi approach once again allowed for the contribution to the joint strength of each control factor and control level, and interactions of the control factors and control levels to be determined. From this analysis and delamination considerations, it was found that numerous small, closely-spaced grooves provided the optimal combination of joint strength in tension and delamination resistance after buckling.

1.2.3 Parameter Selection Stage 3: Final Design

Once the groove optimization designed experiment was completed, a third and final designed experiment was constructed to examine various processing methods to produce the grooves. Additionally, surface finish was once again considered and the use of adhesives was revisited. An additional six configurations were added to the experiment for checking purposes.

Table 1.3 depicts the L18 Orthogonal Array that was constructed for this final investigation. Table 1.4 contains six additional configurations of interest that were included in the experiment. Prototype parts representing the 24 configurations specified in Tables 1.3 and 1.4 were fabricated and evaluated for tensile strength per the procedure used in the previous experiments. Notice that four different processes were considered to produce the grooves both across the grain (cross grooves) and axially—machining (i.e. cutting), grinding, grit blasting, and laser ablation, as well as, a control case of no grooves.

Table 1.3 L18 Orthogonal array for stage 3 (final design)

	1&2	3	4
	A	C	D
	Grooves	Surface finish	Attachment method
1	Smooth	Smooth	Insert mold
2	Smooth	Ground axial fiber exposure	Adhesive assy W/o surface primer
3	Smooth	Laser axial fiber exposure	Adhesive assy W/surface primer
4	Ground axial grooves	Smooth	Insert mold
5	Ground axial grooves	Ground axial fiber exposure	Adhesive assy w/o surface primer
6	Ground axial grooves	Laser axial fiber exposure	Adhesive assy W/ surface primer
7	Ground top-bottom grooves	Smooth	Adhesive assy W/o surface primer
8	Ground top-bottom grooves	Ground axial fiber exposure	Adhesive assy W/ surface primer
9	Ground top-bottom grooves	Laser axial fiber exposure	Insert mold
10	Ground side-side grooves	Smooth	Adhesive assy W/surface primer
11	Ground side-side grooves	Ground axial fiber exposure	Insert mold
12	Ground side-side grooves	Laser axial fiber exposure	Adhesive assy W/o surface primer
13	Laser axial grooves	Smooth	Adhesive assy W/o surface primer
14	Laser axial grooves	Ground axial fiber exposure	Adhesive assy W/ surface primer
15	Laser axial grooves	Laser axial fiber exposure	Insert mold
16	Cut top-bottom grooves	Smooth	Adhesive assy W/ surface primer
17	Cut top-bottom grooves	Ground axial fiber exposure	Insert mold
18	Cut top-bottom grooves	Laser axial fiber exposure	Adhesive assy W/o surface primer

Table 1.4 Six additional configurations of interest

19	Ground cross grooves	Plasma axial fiber exposure	Insert mold
20	Ground cross grooves	Plasma axial fiber exposure	Adhesive assy W/o surface primer
21	Grit blast cross grooves	Smooth	Adhesive assy W/o surface primer
22	Grit blast cross grooves	Laser axial fiber exposure	Insert mold
23	Laser cross grooves	Smooth	Adhesive assy W/o surface primer
24	Laser cross grooves	Laser axial fiber exposure	Insert mold